COBEM 2023 27TH INTERNATIONAL CONGRESS OF MECHANICAL ENGENEERING

ABCM Brazilian Society of Mechanical Sciences and Engineering
27th ABCM International Congress of Mechanical Engineering
December 04-08, 2023, Florianópolis-SC, Brazil

# COB-2023-1327
# ANALYSIS OF RADIATION SHIELDS FOR THE PROTECTION OF POLYMERIC PATCHES EMPLOYED IN FLARE STACKS

**Luiz Cesar Coutinho Junior**
**Robson Felipe Viana da Silva**
Universidade Federal Fluminense. Rua Passo da Pátria, 156, Room 206-D, São Domingos, Niterói, Rio de Janeiro, Brazil
luizcesar@id.uff.br, robsonfelipe@id.uff.br

**Jaqueline Diniz da Silva**
Center for Energy and Petroleum Studies, University of Campinas, Cora Coralina Street, 350, Campinas, São Paulo, Brazil
jdinizz@unicamp.br

**Fabio Toshio Kanizawa**
**Kleber Marques Lisbôa**
**Leandro Alcoforado Sphaier**
Universidade Federal Fluminense. Rua Passo da Pátria, 156, Room 206-D, São Domingos, Niterói, Rio de Janeiro, Brazil
kanizawa@unicamp.br, kmlisboa@id.uff.br, lasphaier@id.uff.br

***Abstract.*** *Polymeric patches are used for quick in situ damage repair of flare stacks, avoiding costly substitutions or long periods of unavailability of the equipment and plant. However, the very nature of the deployment imposes a significant thermal load to these patches due to the surrounding high temperature flames. Radiation shields were specifically designed and experimentally tested with the purpose of evaluating the adequacy of different configurations and development of concepts to avoid overheating of the patch. The experimental apparatus consists of a lidless chamber wherein a sample tube is positioned involved by the patch within radiation shields fixed to its external surface. Two infrared heaters are positioned at the top of the chamber facing the sample and powered with up to 3840 W(e) each to simulate the flames. Thermocouples are positioned in three locations at the base of the patch (below) and another one is fixed to the center of its top side (above); temperature sensors were also fixed to the radiation shields when they are present. A heat flux sensor is employed to monitor the radiation intensity, while an autotransformer is used to control the power delivered to the heaters. A rectified air flow system is installed to continuously renovate the air within the chamber, but mimicking conditions dominated by natural convection. The measurements show that a single shield is already capable of drastically reducing the temperature of the patch, while adding more shields to the stack has a limited benefit. Perforated shields and the associated enhancement of convective heat removal do not compensate the additional radiation flux that is allowed to directly reach the patch through the holes. Radiation shields covering just the patch along the axis of the tube permit a significant amount of radiation to directly reach the patchless portion of the sample, a part of which is conducted to the bottom of the patch overheating it, and thus should be seldom used. Finally, to simulate the aging of the radiation shields, they are coated with high-temperature black paint yielding it significantly less effective at protecting the polymeric patches. The results are expected to guide the design and implementation of thermal protection systems for polymeric repairs, therefore, allowing to reduce the costly maintenance of flare stacks.*

***Keywords:*** *radiation shields, polymeric repair, thermal radiation, high temperature flame*

## 1. INTRODUCTION

The flare tower is a setup used as a safety system in refineries and oil platforms, protecting the facilities and workers in cases of excess pressure in the equipment, hydrocarbon production shutdowns, and gas overproduction. Its burning process occurs at high temperatures, and together with the combustion of toxic gases, it decreases the mechanical resistance of the pipelines and structures near the combustion system, reducing the service life of the structure due to corrosion and pipeline ruptures.

In order to avoid production shutdowns during maintenance procedures, a viable mitigation of the problem is the use of repairs made with polymer composites installed around pipelines that have structural damage.

Among the most employed composites, those comprised of polymer-reinforced fiberglass are highlighted due to cost and ease of manufacturing (Mattos et al., 2014; Budhe et al., 2018; Alabtah et al., 2021).

Studies on the deployment of radiation shields for the thermal protection of polymeric patches for flare towers are scarce. Nevertheless, a proposal involving flat and perforated plates for worker and structural protection was put forward, yielding significant reductions in the radiation flux reaching the protected surface and demonstrating the perforated plates

solution as a viable alternative (Kim et al., 2014). Regarding the design and analysis of such thermal protection systems, much of the work is currently conducted by trial and error due to the lack of testing data on platforms (Kim, 2019). Recent efforts have also addressed this problem numerically by investigating the impact of thermal radiation from flare towers on ground workers (Soni and Parmar, 2018; Lee et al., 2023).

In the literature, authors have used shields and thermal barriers to reduce solar incidence, minimize heat flux generated by flare towers, decrease thermal load within constructions, and reduce temperatures and radiation in test specimens, among others.

Several materials have been employed as thermal barriers in turbine engines, such as zirconium, aiming to mitigate the effect of thermal radiation (Siegel and Spuckler, 1998; Kelly et al., 2006).

In the field of environment and energy, the demand for electricity, both in households and industries, can be significantly reduced through the application of thermal insulation (Mohamed et al., 2016; Pereira, 2016). Additionally, the use of radiation blockers in buildings has proven to be a widely adopted practice to mitigate temperature and control heat flow within them (Costa, 2009; Teh et al., 2017).

In the analysis of macro and microstructure, the effectiveness of spaced shielding in radiation blocking has been duly proven (Cavalcanti, 2011; Muratova et al., 2017).

Therefore, this research aims to contribute to the existing literature on thermal shielding in flare towers.

An experimental investigation of the use of thermal radiation shields for the protection of polymeric repairs of flare stacks is carried out. A cooled chamber comprising a rectified-flow air renewal system and infrared radiators at its top side is used to emulate the radiation flux coming from flames in a flare tower. A properly instrumented tube sample is then positioned inside the chamber for the tests. The effects of the number of shields, perforation of the curved plates, distance from the surface of the tube, and aging are evaluated with the minimization of the temperature within the polymeric patch as the goal.

## 2. EXPERIMENTAL APPARATUS

The system consists of three modules: the test module, the cooling module, and the compressed air module. The test module consists of two square heaters, model Omega QH121260, with an area of 0.09 $m^2$ and a flux of up to 93 $kW/m^2$ each. The heaters are installed in the upper part of the test module with their faces facing downwards and are responsible for imposing heat flux on the outer surface of the sample through radiation. The heaters are powered by an autotransformer (Variac), model JNG - TDGC2 - 20, with a nominal power of up to 20 kVA and 80 A.

The test chamber is composed of metal plates coated with black paint with high thermal absorptivity, preventing overheating effects due to reflection and limiting the incident radiation on the test specimen to that from the heaters. The tube is also part of the setup and is made of API 5L steel. The test module has a length of 1.1 m, width of 0.4 m, and height of 0.6 m, with semi-circular ends of radius 0.2 m. In contact with the external surface of the chamber is the cooling module, where a cold-water coil is installed to cool the walls, and its temperature is controlled by an evaporative cooling tower.

At the base of the test module is the compressed air module, which includes an airflow system. Compressed air is injected into the module through a 15 hp Schulz screw compressor, model Lean SRP 4015, to prevent the heating of the air around the test specimen. This ensures continuous air renewal, regulated by a flow control valve set at 30.96 $m^3/h$. Figure 1 displays the system modules with and without the heaters in the test module.

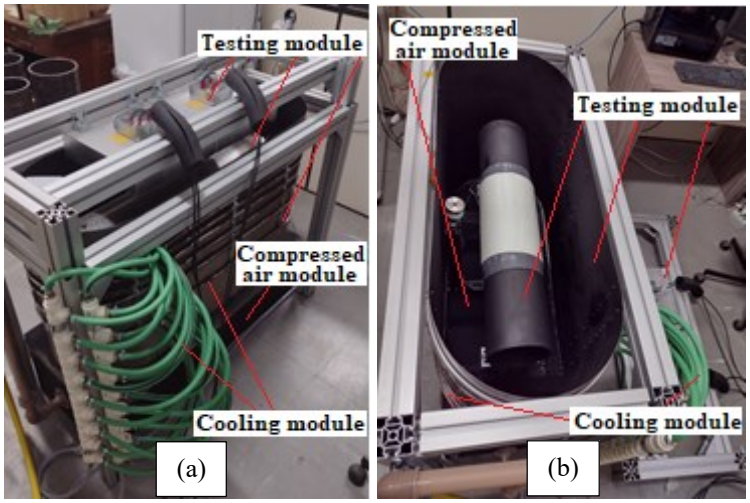


Figure 1. (a) Experimental apparatus and its modules; (b) Experimental apparatus with a view of the chamber interior.

The cooling coil of the chamber is performed with an aluminum serpentine wrapped externally, with a dimension of internal diameter 9.525 mm and 0.80 thick wall, proportionally subdivided based on the distribution of radiant power around the chamber, exhibiting a variation of less than 5°C within the chamber pass. Cooling water flows inside the serpentine provided by an evaporative cooling tower.

The flow sensor, model Hukseflux HF-03/LI19, is positioned below the heater at a vertical distance of 0.15 m and horizontally offset by 0.16 m from the centerline passing through the two heaters. The test specimen is a 6-inch diameter (152.4 mm) API 5L GrB Sch 40 tube, with a length of 0.8 m, similar to the tubes installed in a flare tower, and it is covered by a fiberglass polymer repair, with a length of 0.3 m and a thickness of 6 mm, centered in the middle of the test specimen. Type T thermocouples were installed through holes in the repair region and the tube.

The external circuit includes the heaters, cooling tower, water circuit, compressor, reservoir, filters, lines, and valves.

### 2.1 Radiation shields

The shields are bent at a 180° angle and made of AISI 316L stainless steel, with a length of 0.8 m and a thickness of 1 mm. Four types of shields will be used in this research: plain, perforated, short, and aged shields, as displayed in Figure 2. The radiation shields are supported on the test specimen using clamps, along with spacers and screws. Type T thermocouples are also attached to the central axes of the shields.

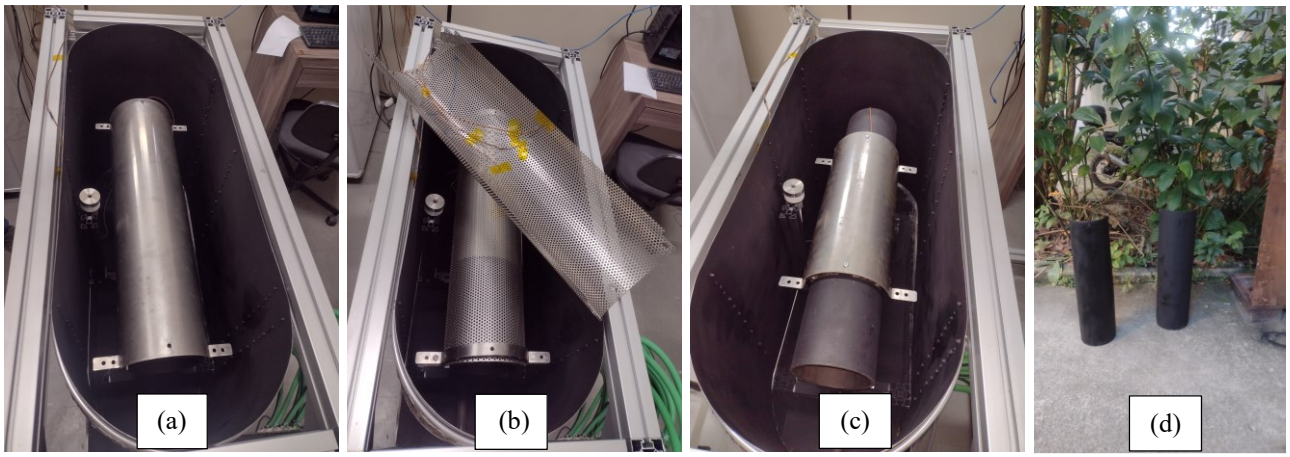


Figure 2. (a) Tube with 1 smooth shielding; (b) Tube with 2 perforated shielding; (c) Tube with 1 short shielding; (d) Shielding coated with high-temperature black paint (Aged shielding).

### 2.2 Thermocouples

The T-type thermocouples are located in the tube and the repair, while the K-type thermocouple is fixed beneath the test specimen, inside the chamber, as displayed in Figure 3. A brief description of the exact thermocouple locations can be found in Table 1.

The thermocouples have been calibrated and have a maximum uncertainty of ± 1.8°C for the K-type thermocouple, which measures the airflow inside the chamber, and ± 2.1°C for the T-type thermocouples, used for measurements on the test specimen, repair, and shields.

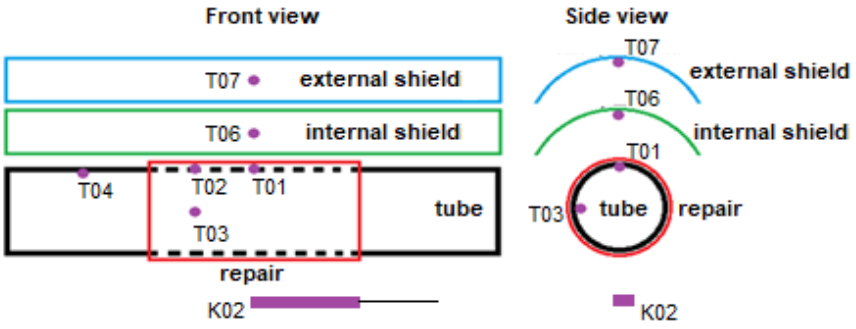


Figure 3. Thermocouple positioning.

Table 1. Description and location of the thermocouples in the configurations.

| **Thermocouples** | **T01** | **T02** | **T03** | **T04** | **T06** | **T07** | **K02** |
|---|---|---|---|---|---|---|---|
| **Location** | Center of the repair | Near the end of the repair | 90° from the top-side | Tube | Internal shield | External shield | Air inside the chamber |

## 3. EXPERIMENTAL PROCEDURE

The configurations are based on parameters such as the type of shield and the tube-shield and shield-shield spacings, with seven configurations defined as shown in Table 2.

Table 2. Characteristics of the experimental configurations.

| **Configuration** | **Distance between Repair and Shielding, mm** | **Distance between the Shieldings, mm** | **Type** |
|---|---|---|---|
| 1 | - | - | Unshielded |
| 2 | 10 | - | Smooth |
| 3 | 10 | 10 | Smooth |
| 4 | 20 | - | Smooth |
| 5 | 10 | 10 | Perforated |
| 6 | 10 | - | Short |
| 7 | 10 | - | Aged |

For each configuration, a minimum of eight measurements are taken, of which at least three are repeated to ensure data accuracy. For each measurement, a voltage is applied to the Variac, thereby defining the value of heat flux generated by the heaters and the experimental heat flux. The experimental heat flux values are approximately 0.5, 1.0, 1.5, 2.0, and 2.5 kW/m$^2$. At each configuration change, either the spacers are replaced, the number of shields is varied, or the tube is changed.

Before starting the experiments, the compressor, water pump, and cooling system are turned on, while ensuring that the airflow control valve is properly set to the defined flow rate. Then, temperature and heat flux data are instantly generated and recorded by the LabView and the LI-19 software, respectively. After the autotransformer is turned on, a voltage value corresponding to the required experimental heat flux is set. The voltage and current are measured by a multimeter, which has an uncertainty of ± 0.8% and ± 2.5% for voltage and current, respectively. While data acquisition is ongoing, from the transient to the steady-state regime, it is important to monitor the temperature increase and its curves to confirm that the data is being acquired correctly. Each acquired measurement takes approximately 3.5 hours to achieve the steady state condition. To confirm the steady state, it is determined that the values obtained from the thermocouples must not vary by more than 0.3°C for 30 minutes. Once the measurement is completed, the data is saved, and another measurement begins by setting a predefined value on the autotransformer.

## 4. RESULTS AND DISCUSSION

The temperature data obtained in the experiment by the thermocouples located on the repair, the tube, the air inside the chamber, and the shields can be observed in the tables below, along with the achieved heat flux values. Figure 4 presents the data for the configuration without radiation shields. The heat flow generated by the heaters ranged from 1.8 to 6.6 kW/m$^2$, and the temperature at the center of the repair varied from 44.8 to 91.2°C. The maximum temperature in the fixture was limited to 100°C during the experiments to prevent material damage.

The data from the shielding configurations are presented in what follows, including smooth long, smooth short, perforated long, and aged long shields. Figure 5 presents the configuration of a smooth shield with a 10 mm spacing. The temperature at the center of the polymeric patch and the heat flow generated by the heaters ranged from 28.6 to 44.2°C and 2.1 to 8.3 kW/m$^2$, respectively. The external shield reached a maximum temperature of 78.1°C, while the minimum temperature was 35.1°C.

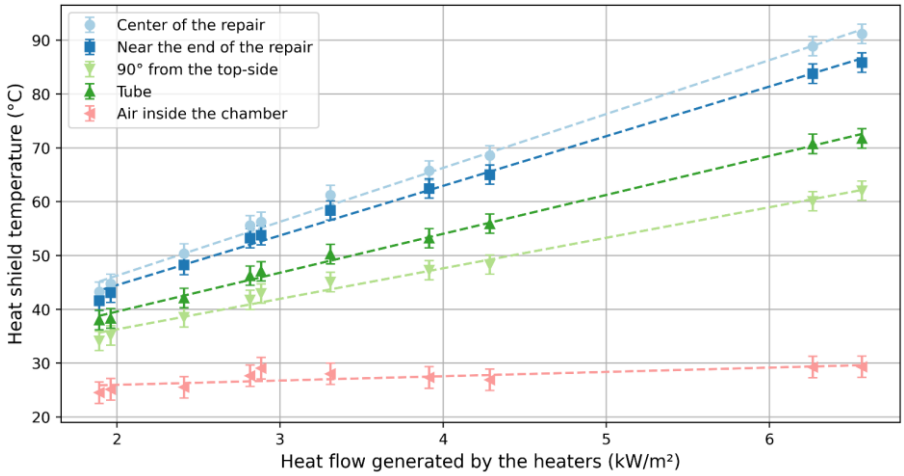


Figure 4. Temperatures for configuration 1 without radiation shields.

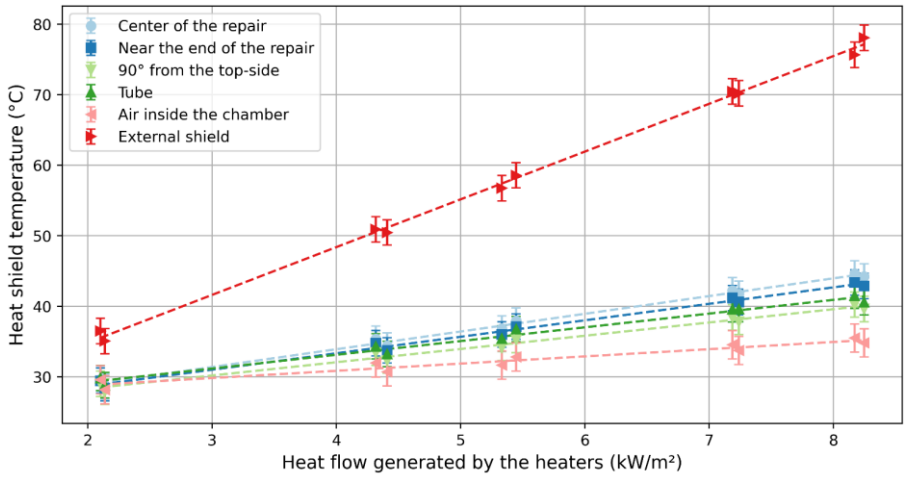


Figure 5. Temperatures of configuration 2 - one smooth shield, spacing of 10 mm.

Configuration 3, in Figure 6, features double shielding, with a spacing of 10 mm between the shields, and between the repair and the shield. The heat flow generated by the heaters ranged from 1.4 to 8.7 kW/m$^2$, reaching a maximum temperature of 29.3°C and a minimum temperature of 22.9°C at the center of the fixture. However, the maximum temperature in the external shield exceeded 100°C due to it being closer to the radiation source than the outer shield in the single-shield configuration.

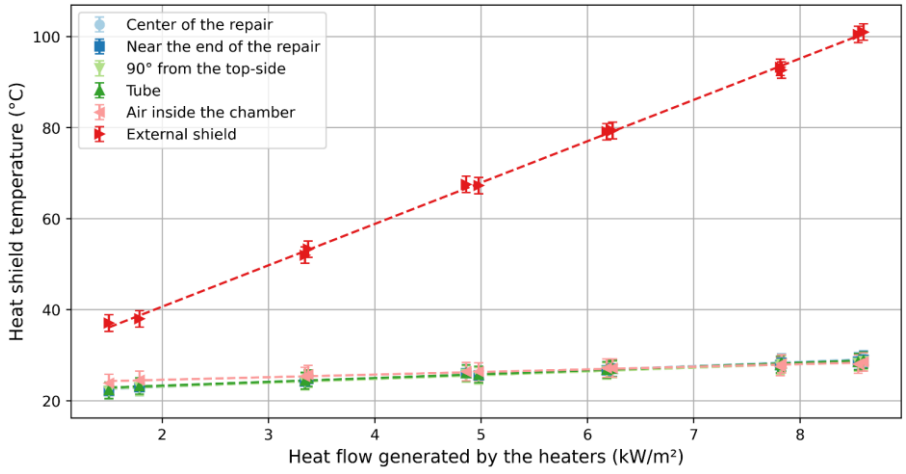


Figure 6. Temperatures of configuration 3 - double smooth shielding, spacing of 10 mm.

The maximum temperature for the configuration with two smooth shields and the maximum temperature for the configuration with one smooth shield were approximately 29°C at the center of the patch, indicating that increasing the number of shields has only a marginal benefit as far as protecting the polymeric repair is concerned.

Continuing with the data for the configurations with smooth shields, Figure 7 shows the configuration with one smooth shield, with a spacing of 20 mm between the patch and the shield, which is 10 mm larger than configuration 2, whose data is available in Figure 5.

In this configuration, the external shield ranged from 36.0 to 76.4°C, resulting from an interval of heat flow generated by the heaters values from 2.2 to 8.7 kW/m$^2$. The temperature at the center of the repair varied by approximately 12°C, with a minimum temperature of 28.8°C and a maximum temperature of 40.1°C.

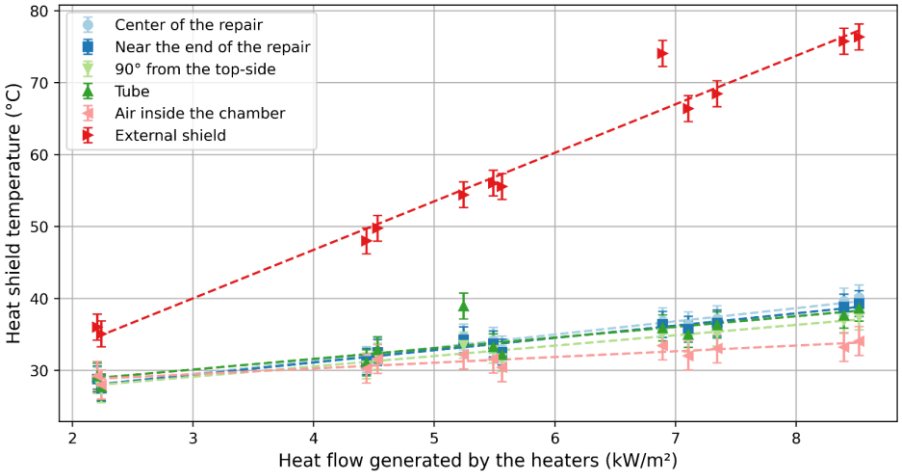


Figure 7. Temperatures of configuration 4 - one smooth shielding, spacing of 20 mm.

The long double perforated shielding, in Figure 8, with a spacing of 10 mm between the repair and shield, and between the two shields, achieved a heat flow generated by the heaters ranging from a minimum of 1.8 kW/m$^2$ to a maximum of 8.0 kW/m$^2$. The temperature within the shield ranged from approximately 40°C to 77°C, establishing a temperature range at the center of the fixture of 26.6 to 40.9°C.

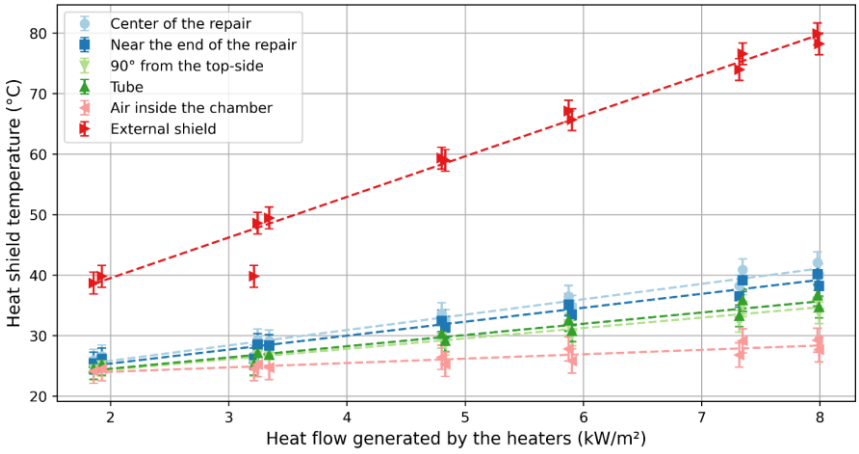


Figure 8. Temperatures of configuration 5 - double perforated shielding, spacing of 10 mm.

The short shield, from configuration 6, in Figure 9, with a 10 mm spacing between the repair and the shield yielded a temperature at the center of the patch that ranged from 39.9 to 51.3°C, and the heat flow generated by the heaters values varied from 2.1 to 9.1 kW/m$^2$. The external shield reached a maximum temperature of 92.8°C.

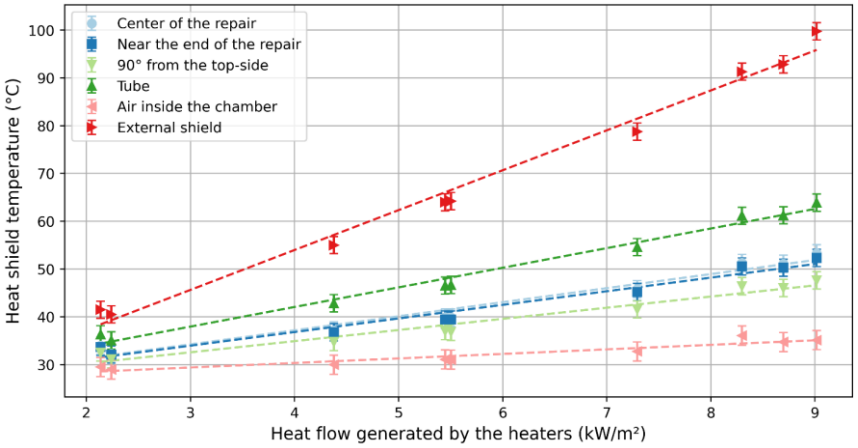


Figure 9. Temperatures of configuration 6 - one short shielding, spacing of 10 mm.

In this latest configuration, utilizing the aged long shield with a spacing of 10 mm between the repair and the shield, it was observed that the temperature of the external shielding exceeded 160°C. On the other hand, the maximum temperature at the center of the patch reached 77.4°C, with the heat flow generated by the heaters ranging from 1.9 to 7.9 kW/m$^2$, as observed in Figure 10.

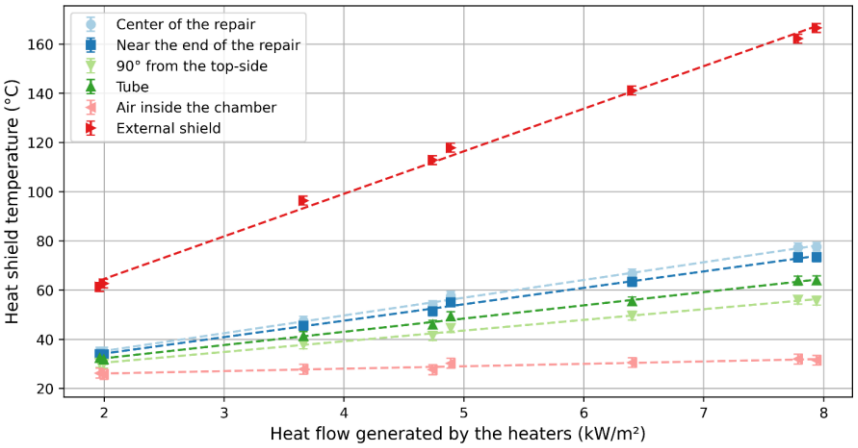


Figure 10. Temperatures of configuration 7 - one aged shield, spacing of 10 mm.

Based on the collected data, it is possible to compare the configurations in terms of the temperatures obtained by the thermocouples and the experimental heat fluxes as well. The results from the experiment are those in which the system reached a steady state, considering only the data saved in the last 10 minutes. The configurations were compared to each other based on the temperature at the center of the repair, as measured by thermocouple 1. The established default configuration was the one without shielding.

Figure 11 compares the configurations without any shield to the cases with a single smooth shield and with a single short shield. The effect of the introduction of just a single shield in terms of the reduction of the temperature of the repair is dramatic, corroborating the efficacy of the developed radiation shields. On the other hand, the difference attested in the comparison between short and long shields is mild and within the experimental uncertainty for most of the range of heat fluxes covered. Nonetheless, the difference becomes significant for the upper portion of the heat flux range, with a short shield showing a poorer capacity to maintain the temperature of the repair low. Such a phenomenon can be attributed to the direct impact of radiation on the uncovered portion of the tube, followed by axial conduction of this heat to the portions of the tube directly underneath the repair, thereby increasing its temperature. Given the relatively low cost of the proposed system, the long shield, covering a significant distance beyond the one occupied by the polymeric patch, is deemed the preferred choice.

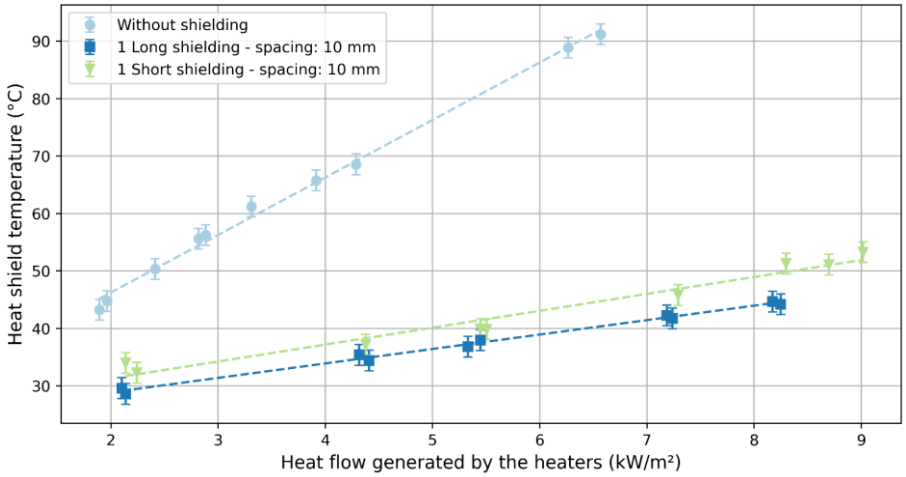


Figure 11. Temperatures in the test specimen - Comparison between long and short shields.

The smooth and aged shields were compared to the configuration without shielding, as shown in Figure 12. The higher absorptivity of the aged shield led to significantly higher temperatures in the repair when compared to the ones attained with the smooth shield. However, the temperatures are still well below the one observed when no radiation shield is installed, building confidence on the capacity of the proposed radiation shield solution to operate in the long-term under harsh conditions.

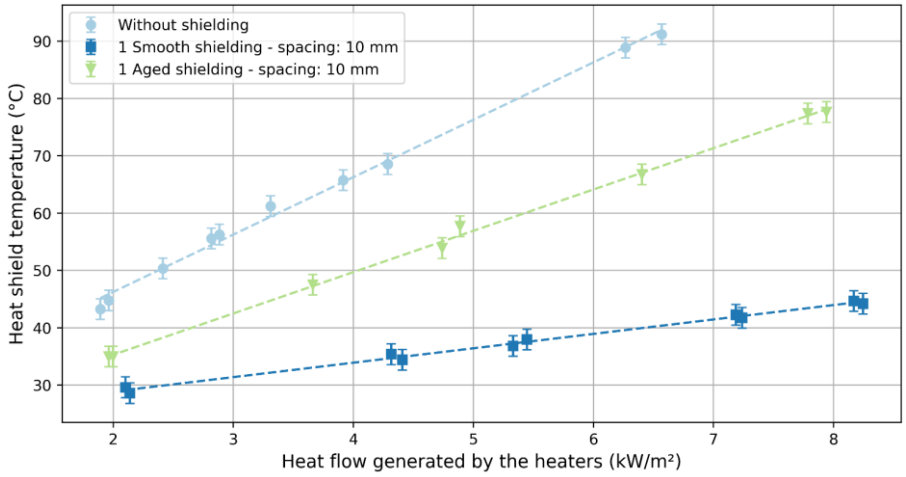


Figure 12. Temperatures in the test specimen - Comparison between smooth shielding and aged shielding.

Figure 13 depicts a comparison between the configurations with 2 radiation shields, either plain or perforated, and the one with no radiation shield. Both solutions can significantly reduce the temperature in the polymeric patch, but with a poorer performance of the perforated-plate-based shield. The rationale behind the use of perforated shields is to leverage the convective heat transfer to enhance the heat removal from the outer surface of the tube. However, the data shows that this effect is not capable of offsetting the collateral effect of having more radiation directly reaching the repair through the holes in the shields.

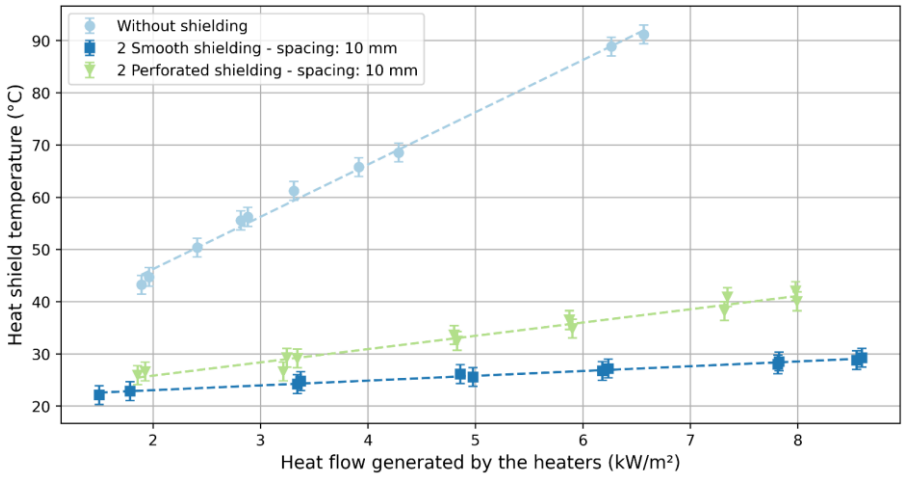


Figure 13. Temperatures in the test specimen - Comparison between double smooth shielding and double perforated shielding.

As depicted in Figure 14, the repair-shield spacing for the smooth shielding configurations with 10 mm and 20 mm can adequately maintain the temperature of the repair within safe limits. However, the influence of the spacing is mild and the difference between the 10 and 20 mm configurations is not statistically significant for most of the tested heat flux range. Still, the configuration employing a more spaced shield consistently yields lower temperatures, which is an effect of the lower axial flow resistance it offers, favoring convective heat removal through air renewal.

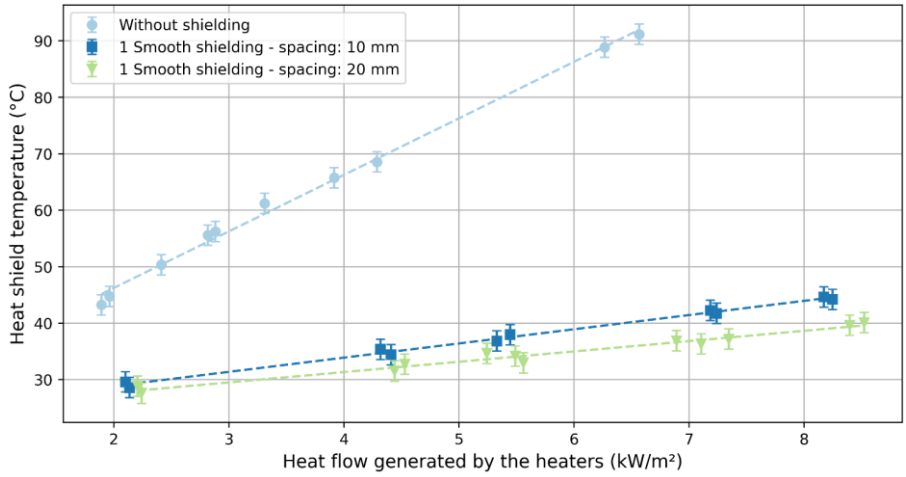


Figure 14. Temperatures in the test specimen - Comparison between long smooth shielding with different spacing.

## 5. CONCLUSION

Based on the conducted studies, certain configurations have proven to be more effective than others in protecting polymeric repairs involving tubes in flare stacks against radiation heat transfer.

Short shields expose a larger portion of the tube to direct radiation that may be conducted to the portion of the tube beneath the polymeric patch, increasing its temperature. Despite this effect being small, the low cost of covering larger tube lengths may favor the conservative design decision to use longer radiation shields spanning at least two times the length of the patch.

Aged shields exhibit high absorptivity, thereby retaining more of the incident radiation and thus passing on a larger amount of thermal energy to polymeric repair. The result is a significant increase in both the temperature of the radiation shield and the patch, although the latter is still significantly lower than what is achieved when no shielding solution is deployed.

Perforated shields, compared to the configurations of aged and short shielding, have shown efficiency, but in comparison to the smooth shielding, they proved to be worse. The most advantageous result was achieved with the configuration of two smooth shields, demonstrating their efficiency in reducing heat transfer to both the tube and the fixture.

## 6. ACKNOWLEDGEMENTS

The authors gratefully acknowledge the Master's scholarship given by CAPES to the first author. This research was funded by Petrobras and supported by The National Agency of Petroleum, Natural Gas and Biofuels, Brazil.

## 7. REFERENCES

Alabtah, F.G., Mahdi, E. and Eliyan, F.F., 2021. "The use of fiber reinforced polymeric composites in pipelines: A review". *Composite Structures*, Vol. 276, pp.001017.

Budhe, S., Banea, M., de Barros, S. and Rohem, N., 2018. Assessment of failure pressure of a gfrp composite repair system for wall loss defect in metallic pipelines. *Materials Science and Engineering Technology*, Vol. 49, pp. 902911.

Cavalcanti, M.A.V., 2011. *Analysis of the influence of reflective surfaces on heat losses in thermal systems (in Portuguese)*. Master's thesis, Graduate Program in Mechanical Engineering, Federal University of Rio Grande do Norte, Natal, Brazil.

Costa, A.F.G.M., 2009. Methodology for designing solar radiation blockers (brises) with a pivotable movable structure for environmental comfort in poultry houses (in Portuguese). *Exacta*, Vol. 7, pp. 013020.

Kelly, M.J., Wolfe, D.E., Singh, J., Eldridge, J., Zhu, D.M. and Miller, R., 2006. "Thermal barrier coatings design with increased reflectivity and lower thermal conductivity for high-temperature turbine applications". *International Journal of Applied Ceramic Technology*, Vol. 3, p. 081093.

Kim, B.J., 2019. "Study on performance of radiant heat shields for offshore installations". *Journal of Ocean Engineering and Technology*, Vol. 33, p.330339.

Kim, S. J., Park, S. I., Lee, J. C., Seo, J. K., Kim, B. J., Ha, Y. C., Paik, J. K. and Heo T. U., 2014. "Experimental study of the reduction of high temperatures and radiation using heat shields associated with flare towers of offshore oil and gas platforms". *Ships and Offshore Structures*, Vol. 9, p. 540549.

Lee, G.N., Jung, K.H., Kim H.J., Kim, B.J., Park, D.K. and Park, Il-R., 2023. "Numerical study of performance of flat and perforated radiant heat shields for offshore structures". *International Journal of Naval Architecture and Ocean Engineering*, Vol. 15, p.001012.

Mattos, H.C., Reis, J., Paim, L., Silva, M., Amorim, F. and Perrut, V., 2014. "Analysis of a glass fibre reinforced polyurethane composite repair system for corroded pipelines at elevated temperatures". *Composite Structures*, Vol. 114, pp. 117123.

Mohamed, H.I., Lee, J. and Chang, J.D., 2016. "The effect of exterior and interior roof thermal radiation on buildings cooling energy". In *International Conference on Sustainable Design, Engineering and Construction – ICSDEC 2016*. Arizona, EUA.

Muratova, E., Matyushkin, L., Moshnikov, V., Chernyakova, K. and Vrublevsky, I., 2017. "Thermal radiation shielding by nanoporous membranes based on anodic alumina". *Journal of Physics: Conference series*, Vol. 872, p. 012020.

Pereira, J.P., 2016. *Development of a ceramic composite to optimize thermal radiation in refractory materials (in Portuguese)*. Professional Master's Thesis, Professional Master's Program in Materials, Oswaldo Aranha Foundation, Volta Redonda, Brazil.

Siegel, R. and Spuckler, C.M., 1998. "Analysis of thermal radiation effects on temperatures in turbine engine thermal barrier coatings". *Materials Science and Engineering A*, Vol. 245, pp. 150159.

Soni, A. and Parmar, N., 2018. "Flare radiation mitigation analysis of onshore oil gas production refining facility for a low cost de-bottlenecking using computer aided techniques". *International Journal of Scientific Engineering Research*, Vol. 9, p. 975982.

Teh, K.S., Yarbrough, D.W., Lim, C.H. and Salleh, E., 2017. "Field evaluation of reflective insulation in south east asia". *Open Engineering*, Vol. 7, p. 352362.

## 8. RESPONSIBILITY NOTICE

The authors are the only responsible for the printed material included in this paper.